Available online at www.eccomasproceedia.org
Eccomas Proceedia SMART (2023) 1088-1099

ECCOMAS
Proceedia

X ECCOMAS Thematic Conference on Smart Structures and Materials
SMART 2023
D.A. Saravanos, A. Benjeddou, N. Chrysochoidis and T. Theodosiou (Eds)

TOWARDS THE ASSESSMENT AND PERFORMANCE QUANTIFICATION OF THE INVERSE PROBLEM FOR VIBRATION-BASED SHM

PEIYUAN ZHOU* **AND FOTIS KOPSAFTOPOULOS†**

*†Intelligent Structural Systems Lab (ISSL)
Rensselaer Polytechnic Institute
110 8^{th} street, Troy, NY 12180, United States
e-mail: *zhoup2@rpi.edu, †kopsaf@rpi.edu

Abstract. The main goal of this work is to investigate and assess the damage state estimation accuracy and robustness (inverse problem) of vibration-based SHM methods based on various stochastic time series representations. The assessment of the models and methods is based on a series of laboratory experiments on a composite wing under different damage states (size and location). An excitation-response time series model with stochastic Functionally Pooled representations is employed and assessed. The inverse estimation problem is investigated in terms of: (i) the model structure employed (exact representation, model order, and functional basis); (ii) parameter estimation method, namely weighted least squares (WLS) and regularized versions to potentially improve generalization and tackle over-fitting; and (iii) loss function of the inverse optimization subproblem.

Key words: Instructions, Smart Structures, Multiphysics Problems, Materials, Computing Methods

1 INTRODUCTION

Engineering structures are subject to many sources of uncertainty; from varying operating/environmental conditions to complex damage evolution, time-varying dynamics, and nonlinear behavior in seemingly identical components. Vibration-based passive- and active-sensing Structural Health Monitoring (SHM) methods form an important family of SHM methods that are oftentimes based on statistical and/or probabilistic metrics and damage sensitive features developed for accurately and robustly analyzing complex structural systems and allowing the extraction of decision confidence intervals. To this end, stochastic time series models and derivative methods have been extensively used within vibration-based SHM to overcome the above challenges. Advantages such as accuracy in modelling system dynamics, robustness against uncertainties, and low data footprint make these models attractive for SHM applications. On the other hand, the damage state estimation task (localization and quantification) constitutes and inverse problem whose effective treatment is dependent on the forward system identification

Peer-review under responsibility of the organizing committee of SMART 2023.
doi: 10.7712/150123.9859.451253

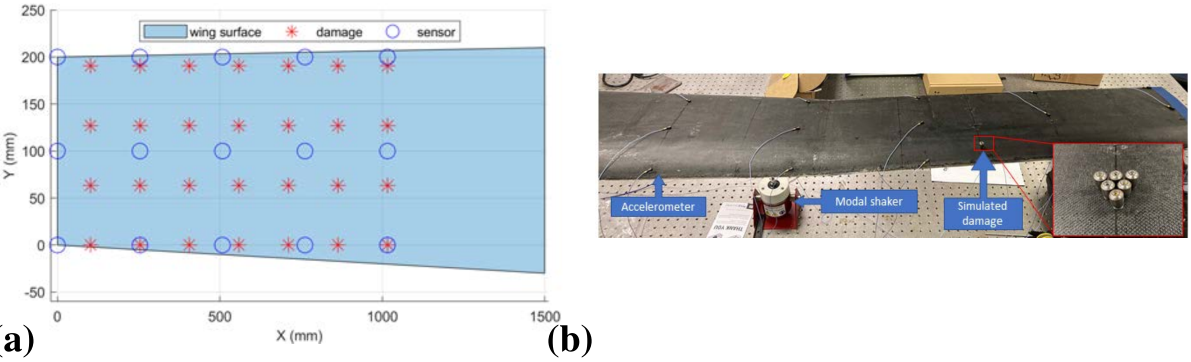

(a) **(b)**

Figure 1: Vibration data is collected from multiple accelerometers on the upper wing surface at locations specified in (a). Incipient damages are simulated by attaching 3 g weights to wing surface using adhesive wax shown in (b) at locations shown as red asterisks.

process (selected model structure, model orders, parameter estimation, and potential hyperparameter tuning) and corresponding statistical properties of the selected model.

Regularization has been used extensively to overcome ill-posed linear inverse problems or to force sparsity when the model suffers poor generalization [1, 2]. Within the framework of linear system identification, regularization posts physically apprehensible effects on model dynamics over time, space, and frequency domains. l^2-norm regularization (i.e. ridge and quadratic) is applied to filter dynamics with small singular values. Ridge regression and quadratic penalties have been applied to state space models for impact force reconstruction [3, 4, 5]. l^1-norm regularization (e.g. LASSO), on the other hand, induces sparsity by eliminating model parameters with a small impact. Sparse model identification techniques have been presented to increase model generalizability and discover true dynamics [6, 7, 8, 9].

In this study, regularization is introduced to improve inverse optimization problem conditions by simplifying the dynamics over damage parameter space, thus improving the robustness and accuracy of damage estimation with limited prior knowledge of the current damage state.

2 VFP-ARX SHM FRAMEWORK

This section introduces the ”global” identification process of damage-affected structural dynamics using Vector-dependent Functionally Pooled (VFP) model integrated with AutoRegressive eXogenous (ARX) time series models, i.e. VFP-ARX, as the wing structure is excited by known white-noise vibration. Via VFP-ARX model constructed using data of a specified damage field, the structural dynamics is captured over a defined range of damage and parameterized with respect to damage parameters (x-location, y-location, size, etc.). The application of VFP-ARX model for global damage estimation has been proven effective in simplified structures and damage conditions [10, 11].

2.1 VFP-ARX model

The estimation of VFP-ARX model follows the system identification process introduced by [12, 13]. Via VFP method, multiple ARX models can be treated as one entity in model identification. The stochasticity in the data set is characterized as time series residual covariance and related to damage state vector $\boldsymbol{k}$ via functional dependency [10]. The general form of VFP-ARX$(na)_p$ model is given by:

$$y_{\boldsymbol{k}}[t] + \sum_{i=1}^{na} a_i \cdot y_{\boldsymbol{k}}[t-i] = \sum_{i=0}^{nb} b_i \cdot x_{\boldsymbol{k}}[t] + e_{\boldsymbol{k}}[t] \qquad e_{\boldsymbol{k}}[t] \sim \text{iid}\mathcal{N}\big(0, \sigma_e^2\big) \tag{1}$$

where $na = nb$ designating the model order, p the number of function basis. with $y_{\boldsymbol{k}}[t]$ the data under various states specified by state vector $\boldsymbol{k} = [k_1,\ k_2, \ldots, k_n]$. $e_{\boldsymbol{k}}[t]$ is the residual (one-step-ahead prediction error) sequence of the model, which is assumed a white (serially uncorrelated) zero mean sequence with variance $\sigma_e^2(\boldsymbol{k})$. $G_j(\boldsymbol{k})$ is the function basis (e.g., Chebyshev, Legendre, Jacobi and etc), where the model parameters $a_i(\boldsymbol{k}), b_i(\boldsymbol{k})$ are modeled as explicit functions of the state vector $\boldsymbol{k}$.

2.2 Model parameter estimation via WLS

The VFP-ARX model of equations is parameterized in terms of the parameter vector to be estimated from the measured signals:

$$\bar{\boldsymbol{\theta}} = [\ a_{1,1}\ a_{1,2}\ \ldots\ a_{i,j}\ b_{1,1}\ b_{1,2}\ \ldots\ b_{i,j} \ \vdots\ \sigma_e^2(\boldsymbol{k})\ ]^T \quad \forall\, \boldsymbol{k} \tag{2}$$

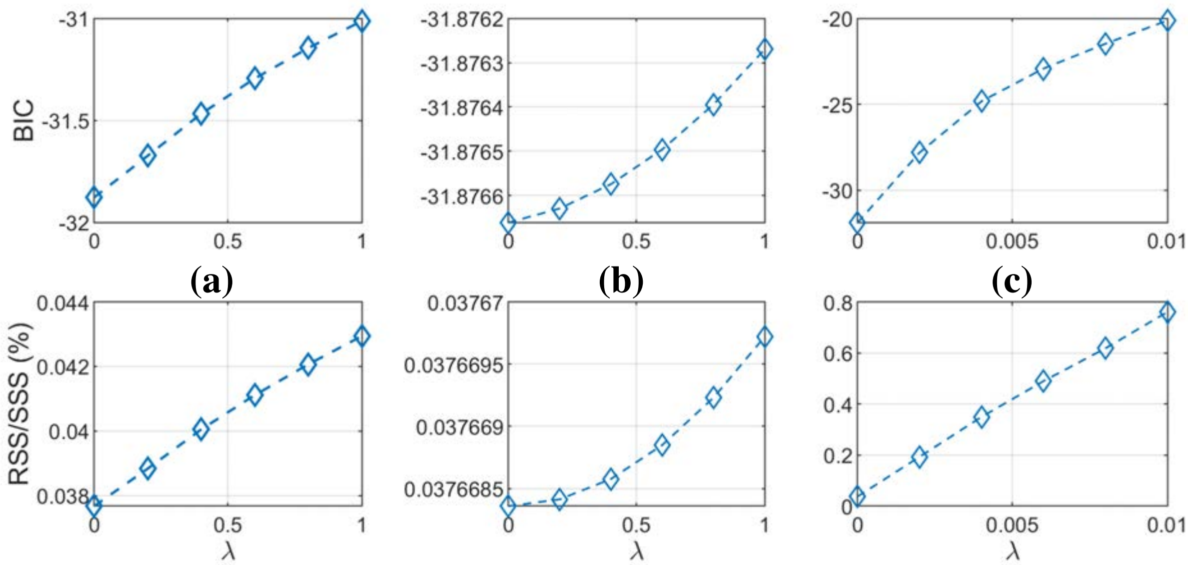

Figure 2: BIC and RSS/SSS(%) are evaluated for FP-ARX$(54)_7$ cases as regularization increases in methods including (a) Ridge, (b) Quadratic, and (c) Lasso.

and may be written in linear regression form at each discrete state:

$$y_{\boldsymbol{k}}[t] = \left[\boldsymbol{\varphi}^T_{\boldsymbol{k}}[t] \otimes \boldsymbol{g}^T(\boldsymbol{k})\right] \cdot \boldsymbol{\theta} + e_{\boldsymbol{k}}[t] = \boldsymbol{\phi}^T_{\boldsymbol{k}}[t] \cdot \boldsymbol{\theta} + e_{\boldsymbol{k}}[t] \tag{3}$$

with:

$$\begin{aligned} \boldsymbol{\varphi}_{\boldsymbol{k}}[t] &:= \Big[-y_{\boldsymbol{k}}[t-1] \; \ldots -y_{\boldsymbol{k}}[t-na] \; u_{\boldsymbol{k}}[t] \; \ldots \; u_{\boldsymbol{k}}[t-nb]\Big]^T_{[(na+nb+1)\times 1]} \\ \boldsymbol{g}(\boldsymbol{k}) &:= \Big[G_1(\boldsymbol{k}) \; \ldots \; G_p(\boldsymbol{k})\Big]^T_{[p\times 1]} \\ \boldsymbol{\theta} &:= \Big[a_{1,1} \; a_{1,2} \; \ldots \; a_{na,p} \; b_{1,1} \; b_{1,2} \; \ldots \; b_{nb,p}\Big]^T_{[((na+nb+1)p\times 1]} \end{aligned} \tag{4}$$

and ^{T} designating transposition and $\otimes$ Kronecker product [14, Chap. 7].

Pooling together the expressions of equation (3) of the VFP-ARX model corresponding to all damage vectors $\boldsymbol{k}$ $(k_{1,1}, k_{1,2}, \ldots, k_{M_1,M_2})$ considered in the experiments and every time step $(t = 1, \ldots, N)$ yields:

$$\boldsymbol{y} = \boldsymbol{\Phi} \cdot \boldsymbol{\theta} + \boldsymbol{e} \tag{5}$$

Gauss-Markov theorem suggests the appropriate criterion to be Weighted Least Squares [15]:

$$J^{\text{WLS}} = \frac{1}{N}\sum_{t=1}^{N} \boldsymbol{e}^T[t]\boldsymbol{\Gamma}^{-1}_{\boldsymbol{e}[t]}\boldsymbol{e}[t] = \frac{1}{N}\boldsymbol{e}^T\boldsymbol{\Gamma}^{-1}_{\boldsymbol{e}}\boldsymbol{e} \tag{6}$$

,which leads to the *Weighted Least Squares (WLS)* estimator:

$$\widehat{\boldsymbol{\theta}}^{\text{WLS}} = \left[\boldsymbol{\Phi}^T\boldsymbol{\Gamma}^{-1}_{\boldsymbol{e}}\boldsymbol{\Phi}\right]^{-1}\left[\boldsymbol{\Phi}^T\boldsymbol{\Gamma}^{-1}_{\boldsymbol{e}}\boldsymbol{y}\right]. \tag{7}$$

In these expressions $\boldsymbol{\Gamma}_{\boldsymbol{e}} = E\{\boldsymbol{e}\boldsymbol{e}^T\}$ ($\boldsymbol{\Gamma}_{\boldsymbol{e}} = \boldsymbol{\Gamma}_{\boldsymbol{e}[t]} \otimes \boldsymbol{I}_N$, with $\boldsymbol{I}_N$ designating the $N \times N$ unity matrix) designates the residual covariance matrix, which is estimated via Ordinary Least Squares. The final residual variance and residual covariance matrix estimates are:

$$\widehat{\sigma}^2_e(\boldsymbol{k}, \widehat{\boldsymbol{\theta}}^{\text{WLS}}) = \frac{1}{N}\sum_{t=1}^{N} e^2_{\boldsymbol{k}}[t, \widehat{\boldsymbol{\theta}}^{\text{WLS}}], \quad \widehat{\boldsymbol{\Gamma}}_{\boldsymbol{e}[t]} = \frac{1}{N}\sum_{t=1}^{N} \boldsymbol{e}[t, \widehat{\boldsymbol{\theta}}^{\text{WLS}}]\boldsymbol{e}^T[t, \widehat{\boldsymbol{\theta}}^{\text{WLS}}] \tag{8}$$

The estimator $\widehat{\boldsymbol{\theta}}^{\text{WLS}}$ may, under mild conditions, be shown to be asymptotically Gaussian distributed with mean at true parameter $\boldsymbol{\theta}^o$ and covariance matrix $\boldsymbol{P}_{\boldsymbol{\theta}}$:

$$\widehat{\bar{\boldsymbol{\theta}}}^{\text{WLS}} \sim \mathcal{N}(\bar{\boldsymbol{\theta}}_0, \boldsymbol{P}^{ML}), as \quad N \to \infty \tag{9}$$

2.3 Inverse estimation of damage parameter

Damage estimation is based on an inverse optimization process in terms of damage vector $\boldsymbol{k}$ and $\sigma_e^2(\boldsymbol{k})$ with respect to an unknown excitation and response signal. As the model is re-parameterized by damage vector ($\boldsymbol{k}$) rather than projection coefficient ($\boldsymbol{\theta}$):

$$\mathcal{M}^{\mathcal{V}}(\boldsymbol{k}, \sigma_e^2(\boldsymbol{k})) : y[t] + \sum_{i=1}^{na} a_i(\boldsymbol{k}) \cdot y[t-i] = \sum_{i=0}^{nb} b_i(\boldsymbol{k}) \cdot x[t-i] + e[t], \tag{10}$$

The estimation of current $\boldsymbol{k}$ and $\sigma_e^2(\boldsymbol{k})$ based on unknown signal $y(t)$ and $x(t)$ can be realized through the following non-linear least square (NLS) and variance estimator.

$$\widehat{\boldsymbol{k}} = \arg \min_{\boldsymbol{k} \in \mathbf{R}^m} \sum_{i=1}^{N} e_u^T[t, \boldsymbol{k}] e_u[t, \boldsymbol{k}] \ , \quad \sigma_u^2(\widehat{\boldsymbol{k}}) = \frac{1}{N} \sum_{t=1}^{N} e_u[t, \widehat{\boldsymbol{k}}] e_u^T[t, \widehat{\boldsymbol{k}}] \tag{11}$$

The estimation of $\widehat{k}$ is realized via a two-step process of generic algorithm (GA) and sequential quadratic programming (SQP) optimization. As GA searches through the entire damage space, the SQP improves on the accuracy of finding the exact global optimum $\widehat{k}$.

3 REGULARIZED WEIGHTED LEAST SQUARE ESTIMATION

Regularization is introduced to reduce over-fitting in model parameters estimation, where three methods, Ridge, Quadratic, and Lasso are evaluated for both FP-ARX and VFP-ARX cases. The estimators and statistical properties of these regularization methods for WLS estimation of (V)FP-ARX model parameters ($\widehat{\boldsymbol{\theta}}$) are formulated.

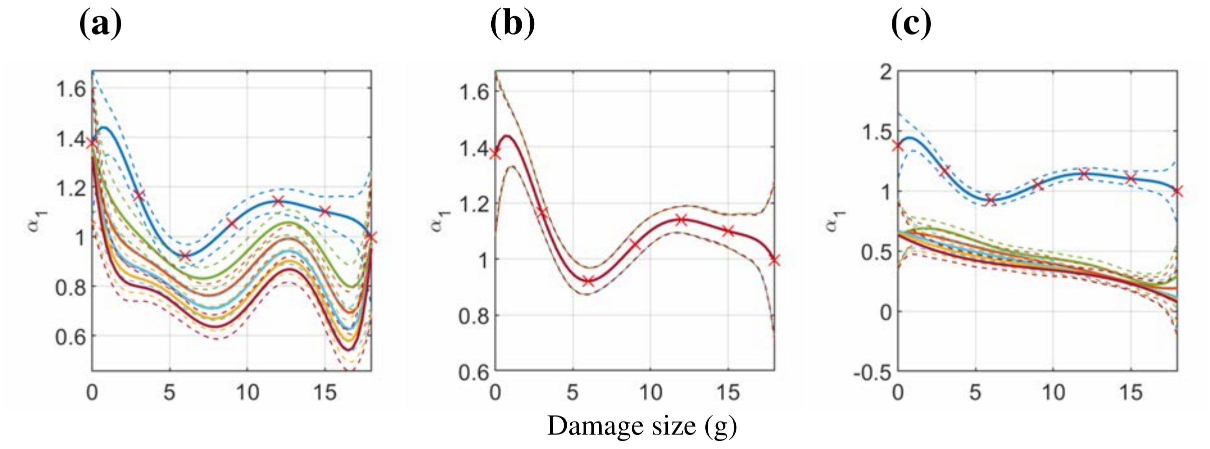

Figure 3: Model parameters [α_1,α_2,α_3,α_4,] and their 95% $C.I.$ (plotted as dotted lines in corresponding color) are evaluated for $FP{-}ARX(54)_7$ cases as regularization increases in methods including: (a) Ridge, (b) Quadratic,and (c) Lasso. Parameter from individually estimated ARX models are shown as red '$\times$'.

3.1 Quadratic and Ridge

Quadratic regularization introduces the penalty term J^{Quad} as a quadratic function of $\boldsymbol{\theta}$. Thus the problem is formulated as:

$$\widehat{\boldsymbol{\theta}}^{quad} = \arg\min_{\boldsymbol{\theta}} \frac{1}{NM_1M_2}\boldsymbol{e}^T\boldsymbol{\Gamma}_{\boldsymbol{e}}^{-1}\boldsymbol{e} + \lambda\boldsymbol{\theta}^T\boldsymbol{P}^{-1}\boldsymbol{\theta} \tag{12}$$

,where $\boldsymbol{P}$ is the regularization matrix and λ is regularization parameter. In the case when $\boldsymbol{P}$ is singular, Moore-Penrose pseudoinverse is used instead, designated as P^+, making the quadratic penalty $\lambda\boldsymbol{\theta}^T\boldsymbol{P}^+\boldsymbol{\theta}$. Then, the closed-form WLS-quadratic estimator is obtained as follows.

$$\widehat{\boldsymbol{\theta}}^{quad} = \left[\boldsymbol{P}\boldsymbol{\Phi}^T\boldsymbol{\Gamma}_{\boldsymbol{e}}^{-1}\boldsymbol{\Phi} + n\lambda\boldsymbol{I}_n\right]^{-1}\left[\boldsymbol{P}\boldsymbol{\Phi}^T\boldsymbol{\Gamma}_{\boldsymbol{e}}^{-1}\boldsymbol{y}\right], \quad n = NM_1M_2 \tag{13}$$

Assuming a deterministic regression matrix $\boldsymbol{\Phi}$ and white-noise residual $e[t]$, the statistical properties of wls-quadratic estimator are obtained below: [1]

$$E(\widehat{\boldsymbol{\theta}}^{quad}) = \left[\boldsymbol{\Phi}^T\boldsymbol{\Gamma}_{\boldsymbol{e}}^{-1}\boldsymbol{\Phi} + n\lambda\boldsymbol{P}^{-1}\right]^{-1}\left[\boldsymbol{\Phi}^T\boldsymbol{\Gamma}_{\boldsymbol{e}}^{-1}\boldsymbol{\Phi}\boldsymbol{\theta}_0\right] \tag{14}$$

$$\widehat{\boldsymbol{\theta}}^{quad}_{bias} = -\left[\boldsymbol{\Phi}^T\boldsymbol{\Gamma}_{\boldsymbol{e}}^{-1}\boldsymbol{\Phi} + n\lambda\boldsymbol{P}^{-1}\right]^{-1}\left[\lambda\boldsymbol{P}^{-1}\boldsymbol{\theta}_0\right] \tag{15}$$

$$Cov(\widehat{\boldsymbol{\theta}}^{quad}, \widehat{\boldsymbol{\theta}}^{quad}) = \left[\boldsymbol{\Phi}^T\boldsymbol{\Gamma}_{\boldsymbol{e}}^{-1}\boldsymbol{\Phi} + n\lambda\boldsymbol{P}^{-1}\right]^{-1}\widehat{\boldsymbol{\sigma}}_e^2\boldsymbol{\Phi}^T\boldsymbol{\Gamma}_{\boldsymbol{e}}^{-1}\boldsymbol{\Phi}\left[\boldsymbol{\Phi}^T\boldsymbol{\Gamma}_{\boldsymbol{e}}^{-1}\boldsymbol{\Phi} + n\lambda\boldsymbol{P}^{-1}\right]^{-1} \tag{16}$$

$$MSE(\widehat{\boldsymbol{\theta}}^{quad}, \boldsymbol{\theta}_0) = Cov(\widehat{\boldsymbol{\theta}}^{quad}, \widehat{\boldsymbol{\theta}}^{quad}) + \widehat{\boldsymbol{\theta}}^{quad}_{bias}(\widehat{\boldsymbol{\theta}}^{quad}_{bias})^T \tag{17}$$

,where $\boldsymbol{P}_{optimal} = \boldsymbol{\theta}_0\boldsymbol{\theta}_0^T$ when $MSE(\widehat{\boldsymbol{\theta}}^{quad}, \boldsymbol{\theta}_0)$ is minimized. In this case, the regularization matrix is assumed to be $\boldsymbol{P}_0 = \widehat{\boldsymbol{\theta}}^{\text{WLS}}(\widehat{\boldsymbol{\theta}}^{\text{WLS}})^T$ since true model parameter $\boldsymbol{\theta}_0$ is unknown. When

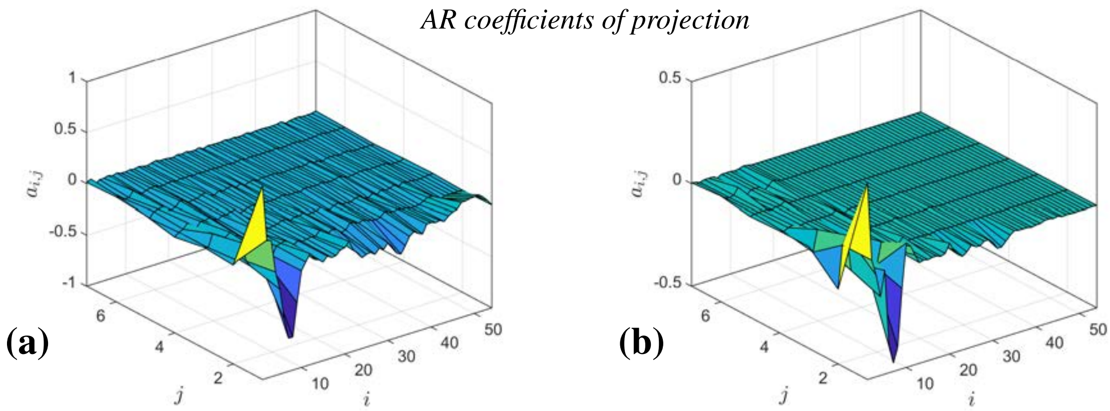

Figure 4: In the case of FP-ARX$(54)_7$, coefficient of projection ($\widehat{\boldsymbol{\theta}} = [a_{i,j} \vdots b_{i,j}]$) is shown to be gradually reduced to zero as Lasso regularization parameter (λ) increases: (a) $\lambda = 0$, and (b) $\lambda = 0.002$

the $\boldsymbol{P}$ is defined to be $\boldsymbol{I}_n$, the formulation correspond to the special case of WLS-ridge that is formulized as:

$$\widehat{\boldsymbol{\theta}}^{ridge} = \arg\min_{\boldsymbol{\theta}} \frac{1}{NM_1M_2}\boldsymbol{e}^T\boldsymbol{\Gamma}_{\boldsymbol{e}}^{-1}\boldsymbol{e} + \lambda\boldsymbol{\theta}^T\boldsymbol{I}\boldsymbol{\theta} \tag{18}$$

The estimator is reduced to:

$$\widehat{\boldsymbol{\theta}}^{ridge} = \left[\boldsymbol{\Phi}^T\boldsymbol{\Gamma}_{\boldsymbol{e}}^{-1}\boldsymbol{\Phi} + n\lambda\boldsymbol{I}_n\right]^{-1}\left[\boldsymbol{\Phi}^T\boldsymbol{\Gamma}_{\boldsymbol{e}}^{-1}\boldsymbol{y}\right], \quad n = NM_1M_2 \tag{19}$$

3.2 Lasso

Least absolute shrinkage and selection operator (LASSO) posts an l^1-norm on the coefficient of projection ($\boldsymbol{\theta}$) that effectively reduces some entries to zero. The WLS-LASSO problem is formulated as:

$$\widehat{\boldsymbol{\theta}}^{LASSO} = \arg\min_{\boldsymbol{\theta}} \frac{1}{NM_1M_2}\boldsymbol{e}^T\boldsymbol{\Gamma}_{\boldsymbol{e}}^{-1}\boldsymbol{e} + \lambda||\boldsymbol{\theta}||_1 \tag{20}$$

The estimation is done via the coordinate descent algorithm [16]. Due to the non-linear and non-differentiable problem formulation, the statistical properties of the LASSO estimator is provided by a quadratic approximation that writes $||\boldsymbol{\theta}||_1$ as $\sum_i^{p(na+nb)} \theta_i^2/|\theta_i|$ [17, 2].

$$E(\widehat{\boldsymbol{\theta}}^{LASSO}) = \left[\boldsymbol{\Phi}^T\boldsymbol{\Gamma}_{\boldsymbol{e}}^{-1}\boldsymbol{\Phi} + \lambda\boldsymbol{W}^-\right]^{-1}\left[\boldsymbol{\Phi}^T\boldsymbol{\Gamma}_{\boldsymbol{e}}^{-1}\boldsymbol{\Phi}\boldsymbol{\theta}_0\right] \tag{21}$$

$$Cov[\widehat{\boldsymbol{\theta}}^{LASSO}, \widehat{\boldsymbol{\theta}}^{LASSO}] = \left[\boldsymbol{\Phi}^T\boldsymbol{\Gamma}_{\boldsymbol{e}}^{-1}\boldsymbol{\Phi} + \lambda\boldsymbol{W}^-\right]^{-1}\boldsymbol{\Phi}^T\boldsymbol{\Gamma}_{\boldsymbol{e}}^{-1}\boldsymbol{\Phi}\left[\boldsymbol{\Phi}^T\boldsymbol{\Gamma}_{\boldsymbol{e}}^{-1}\boldsymbol{\Phi} + \lambda\boldsymbol{W}^-\right]^{-1}\widehat{\boldsymbol{\sigma}}_e^2 \tag{22}$$

W^- designates the generalized inverse of a diagonal matrix with $W_{ii}^- = |\widehat{\boldsymbol{\theta}}_i(\lambda)|^{-1}$.

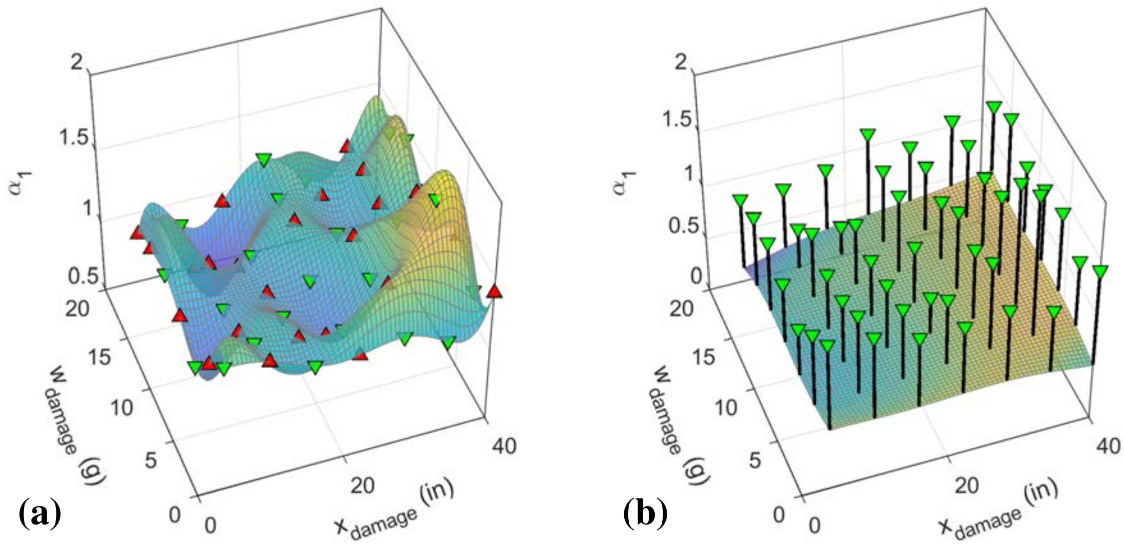

Figure 5: In the case of VFP-ARX$(54)_{49}$, model parameters α_1 are evaluated as regularization increases from (a)$\lambda = 0$ to (b)$\lambda = 0.002$. Parameters from individually estimated ARX models are shown as 'Δ'

4 RESULTS AND ANALYSIS

4.1 FP cases

Fig.2 shows the model selection criteria: Bayesian Information Criterion (BIC) and Residual Sum of Square/Signal Sum of Square (RSS/SSS) reflecting the changes in model complexity and accuracy as regularization parameter (λ) increases. For the 2-norm regularization, *i.e.*Quadratic and Ridge, Ridge posts a more aggressive regularization than Quadratic given the problem formulation in Equation (12)(18). This shows that the regularization matrix $\boldsymbol{P}$ dominates the quadratic penalty term in eqn.12 as its inverse $\boldsymbol{P}^{-1}$ (or $\boldsymbol{P}^{+}$) is numerically small when compare to $\boldsymbol{I}_n$ in ridge regularization. In the case of LASSO regularization, regularization takes effect quickly with a small increase in λ.

A direct examination of ARX parameter ($a_1,\ a_2,\ a_3$) is shown in Fig. 3, which reflects the effect of regularization on FP-ARX model dynamics. With a complete 7^{th} degree functional basis, parameters estimated via unregularized WLS ($\lambda = 0$) coincide with independently estimated ARX parameters shown with red '$\times$'. As λ increases, LASSO regularization smooths the variation of ARX parameter with respect to increasing damage size. On the other hand, the quadratic regularization penalty, Ridge and Quadratic, is less effective when the regularization parameter is kept at a similar level. Taking a direct look at the coefficient of projection $\widehat{\boldsymbol{\theta}} = [a_{i,j} \vdots b_{i,j}]$ estimated via LASSO-WLS, Fig. 4 shows the minor parameters discriminated in the process of regularization, thus creating a sparse dynamic model.

4.2 VFP cases

As the comparison of regularization methods has shown in FP cases, forcing a sparse model with LASSO is the most effective in altering the model residual ($e_{\boldsymbol{k}}$). The same LASSO-WLS is applied to VFP cases with a 2-dimension damage vector parameterizing both damage size and

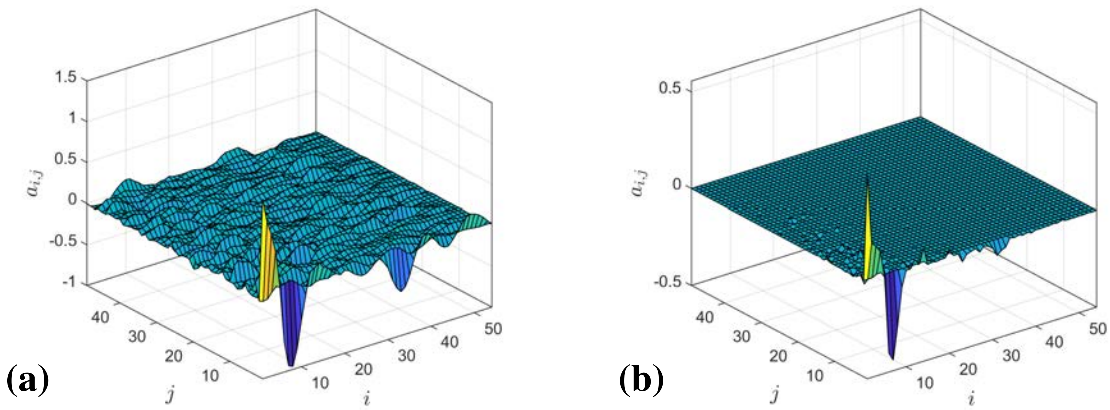

Figure 6: In the case of VFP-ARX$(54)_{49}$, coefficient of projection ($\widehat{\boldsymbol{\theta}} = [a_{i,j} \vdots b_{i,j}]$) is shown to be gradually reduced to zero as Lasso regularization parameter (λ) increases: (a) $\lambda = 0$, and (b) $\lambda = 0.002$

damage x-location. BIC and RSS in Fig. 2 shows the effect of LASSO comparable to that of FP cases. Sparsity is enforced on the coefficient of projection ($\boldsymbol{\theta}$) as it is shown in Fig. 6. The effect of higher order basis (j) and higher ARX orders (i) are alleviated. Consequently, simplification of VFP model dynamic is observed in characteristic ARX model parameters (α_1 and α_2) that is

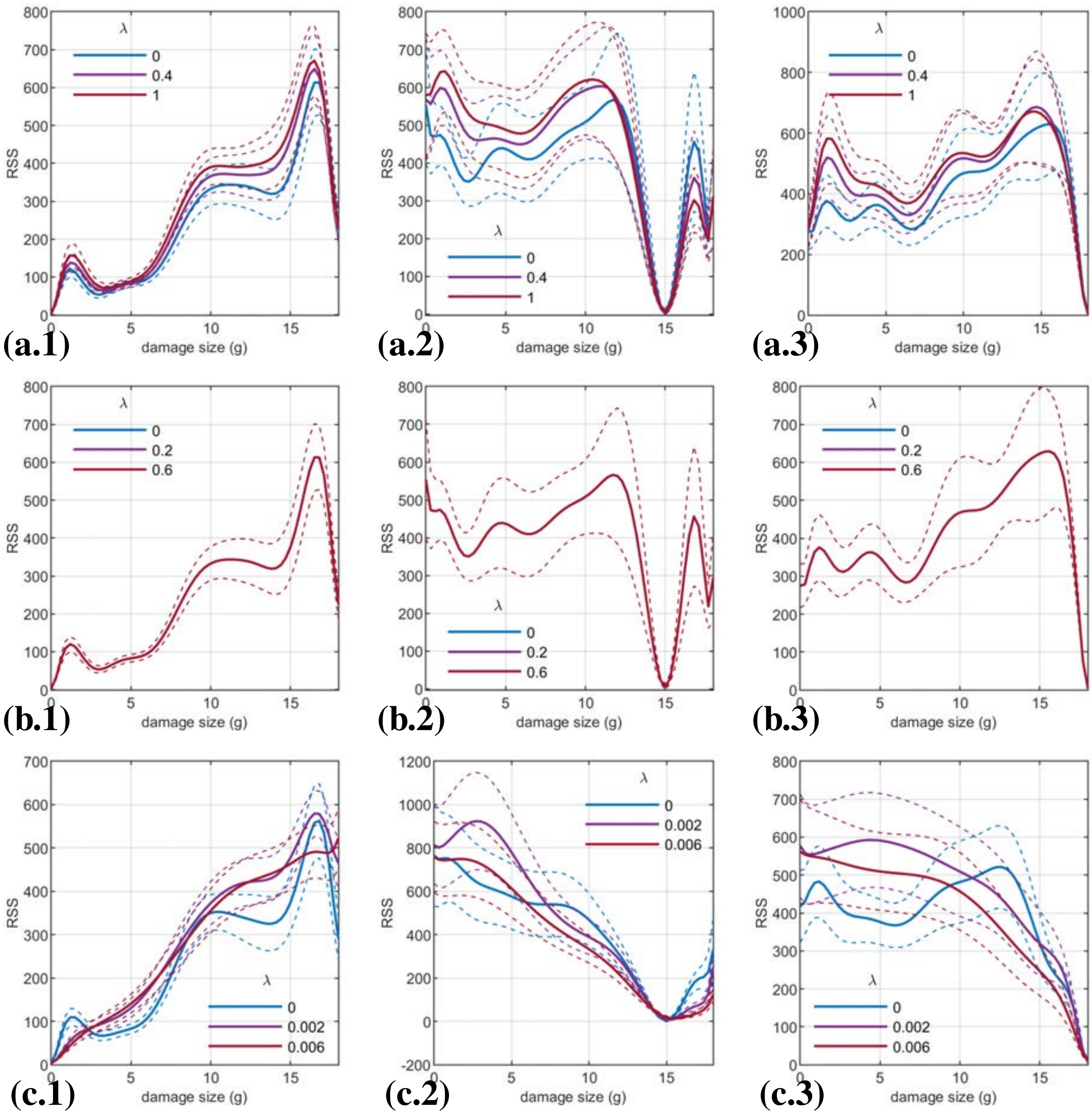

Figure 7: In the case of FP-ARX$(54)_7$, the loss functions of inverse estimation formulation parameterized by damage size and damage x-location are shown with 2 *stds* (shown by dotted lines): (a.1)-(a.3) Ridge regularization at (damage size$= 0, 15, 18$g), (b.1)-(b.3) Quadratic regularization at (damage size$= 0, 15, 18$g), (c.1)-(c.3) LASSO regularization at (damage size$= 0, 15, 18$g)

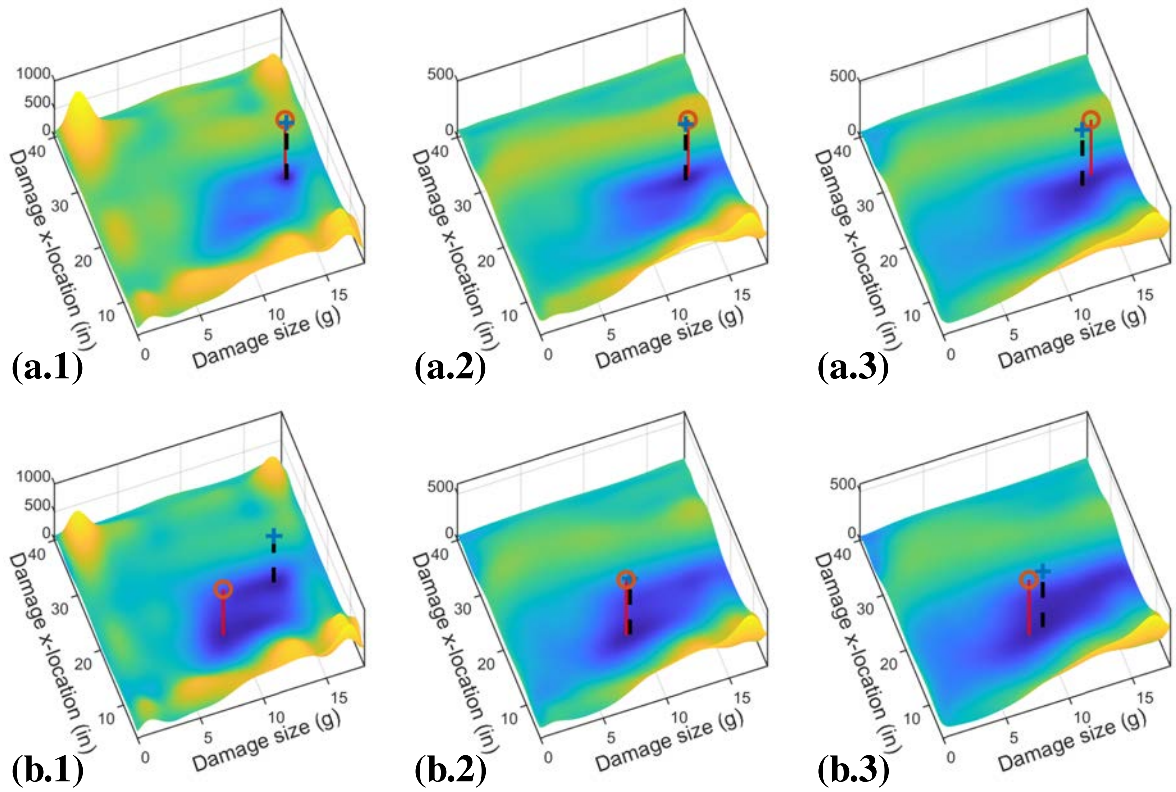

Figure 8: In the case of VFP-ARX$(54)_{49}$, the loss functions of inverse estimation w.r.t damage state. (a.1)-(a.3) damage [$x = 20\ in$, $w = 15\ g$] with λ=0, 2e-4, 6e-4, (b.1)-(b.3) damage [$x = 16\ in$, $w = 9\ g$] with λ=0, 2e-4, 6e-4. Red 'o' shows the true damage state and blue '+' shows the true global minimum.

shown in Fig. 3.

4.3 Model residual distribution

As the residual-based state estimation outcome depends directly on the distribution of loss function (RSS) over the damage parameter space, it is expected that regularization would alter the residual RSS distribution to overcome over-fitting and introduce robustness over stochastic test data. Fig. 7 and 8 exhibit the change of loss function over increasing regularization. In simplified FP cases, Fig. 7(b) shows quadratic regularization has little effect over the loss function as the model parameter varies little with low regularization parameter. Fig. 7(a)(c) shows both ridge and LASSO have the capability to eliminate local minimums. But lasso is more sensitive to hyperparameter tuning, as a preferable loss function condition is achieved when $\lambda = 0.006$.

The same effect of LASSO on loss function is shown in VFP cases, which has a 2-D loss function. Fig. 8 shows two representative damage cases when test-data-induced loss functions have local minimums that clutter the global minimums (Fig. 8(a.1) and have global minimums identified to false damage state (Fig. 8(b.1)). Applying LASSO regularization simplifies the loss function surface, which reduces the burden on the optimization process. Also, Fig. 8(b.2)(b.3) shows the regularization increases the model robustness under test data by moving the global minimum to actual damage.

5 CONCLUSIONS

This research is purposed to evaluate the effect of regularization on (V)FP-ARX-based inverse estimation global SHM method. Ridge, Quadratic and LASSO methods are compared over an FP-ARX model of increasing damage at a fixed location. The LASSO regularization is observed to be the most sensitive to hyperparameter tuning. Then, the LASSO regularization is applied to a VFP-ARX model trained with varying damage sizes along the wing span. It is observed that the loss function of inverse damage estimation has a better condition for damage parameter optimization when regularization is applied to induce model sparsity. In future research, topics will be explored such as the quantification of regularization bias and variance, tuning of hyperparameter towards convexity in loss function of inverse estimation, and a bayesian damage quantification process based on model residuals.

REFERENCES

[1] *Regularized System Identification: Learning Dynamic Models from Data*.

[2] R. Tibshirani, “Regression shrinkage and selection via the lasso,” *Journal of the Royal Statistical Society. Series B (Methodological)*, vol. 58, no. 1, pp. 267–288, publisher: [Royal Statistical Society, Wiley]. [Online]. Available: https://www.jstor.org/stable/2346178

[3] J. Liu, B. Qiao, Y. Wang, W. He, and X. Chen, “Non-convex sparse regularization via convex optimization for impact force identification,” *Mechanical Systems and Signal Processing*, vol. 191, p. 110191. [Online]. Available: https://www.sciencedirect.com/science/article/pii/S0888327023000985

[4] Y. Liu and L. Wang, “A two-step weighting regularization method for stochastic excitation identification under multi-source uncertainties based on response superposition-decomposition principle,” *Mechanical Systems and Signal Processing*, vol. 182, p. 109565. [Online]. Available: https://www.sciencedirect.com/science/article/pii/S0888327022006604

[5] M. Aucejo, O. De Smet, and J. F. Deü, “On a space-time regularization for force reconstruction problems,” *Mechanical Systems and Signal Processing*, vol. 118, pp. 549–567. [Online]. Available: https://www.sciencedirect.com/science/article/pii/S0888327018306125

[6] R. Fuentes, R. Nayek, P. Gardner, N. Dervilis, T. Rogers, K. Worden, and E. J. Cross, “Equation discovery for nonlinear dynamical systems: A bayesian viewpoint,”

Mechanical Systems and Signal Processing, vol. 154, p. 107528. [Online]. Available: https://www.sciencedirect.com/science/article/pii/S0888327020309146

[7] Y. Chen, X. Liang, and M. J. Zuo, "Sparse time series modeling of the baseline vibration from a gearbox under time-varying speed condition," *Mechanical Systems and Signal Processing*, vol. 134, p. 106342. [Online]. Available: https://www.sciencedirect.com/science/article/pii/S0888327019305631

[8] Y. Chen and M. J. Zuo, "A sparse multivariate time series model-based fault detection method for gearboxes under variable speed condition," *Mechanical Systems and Signal Processing*, vol. 167, p. 108539. [Online]. Available: https://www.sciencedirect.com/science/article/pii/S0888327021008803

[9] Y. Chen, S. Schmidt, P. S. Heyns, and M. J. Zuo, "A time series model-based method for gear tooth crack detection and severity assessment under random speed variation," *Mechanical Systems and Signal Processing*, vol. 156, p. 107605. [Online]. Available: https://www.sciencedirect.com/science/article/pii/S0888327020309912

[10] F. P. Kopsaftopoulos and S. D. Fassois, "A stochastic functional model based method for vibration based damage detection, localization, and magnitude estimation," *Mechanical Systems and Signal Processing*, vol. 39, no. 1–2, pp. 143–161, August–September 2013.

[11] P. Zhou and F. Kopsaftopoulos, "Damage localization and magnitude estimation on a composite UAV wing via stochastic functionally pooled models," *STRUCTURAL HEALTH MONITORING 2021*, no. 0, number: 0. [Online]. Available: http://www.dpi-proceedings.com/index.php/shm2021/article/view/36240

[12] L. Ljung, *System Identification: Theory for the User*, 2nd ed. Prentice–Hall, 1999.

[13] T. Söderström and P. Stoica, *System Identification*. Prentice–Hall, 1989.

[14] D. Bernstein, *Matrix Mathematics*. Princeton University Press, 2005.

[15] W. H. Greene, *Econometric Analysis*, 5th ed. Prentice–Hall, 2003.

[16] J. H. Friedman, T. Hastie, and R. Tibshirani, "Regularization paths for generalized linear models via coordinate descent," vol. 33, pp. 1–22. [Online]. Available: https://doi.org/10.18637/jss.v033.i01

[17] M. R. Osborne and B. A. Turlach, "On the lasso and its dual," *Journal of Computational and Graphical Statistics*, vol. 9, no. 2, pp. 319–337. [Online]. Available: http://www.jstor.org/stable/1390657